



**HELMHOLTZ
ZENTRUM FÜR
INFEKTIONSFORSCHUNG**

**This is an by copyright after embargo allowed publisher's PDF of an article
published in**

**Horstmann, N., Essig, S., Bockelmann, S., Wieczorek,
H., Huss, M., Sasse, F., Menche, D.**

**Archazolid A-15-O- β -D-glucopyranoside and iso-
archazolid B: Potent V-ATPase inhibitory polyketides
from the Myxobacteria cystobacter violaceus and
Archangium gephyra**

**(2011) Journal of Natural Products, 74 (5), pp. 1100-
1105.**

Archazolid A-15-O- β -D-glucopyranoside and *iso*-Archazolid B: Potent V-ATPase Inhibitory Polyketides from the Myxobacteria *Cystobacter violaceus* and *Archangium gephyra*

Nicole Horstmann,[†] Sebastian Essig,[†] Svenja Bockelmann,[§] Helmut Wieczorek,[§] Markus Huss,[§] Florenz Sasse,^{||} and Dirk Menche^{*,†,‡}

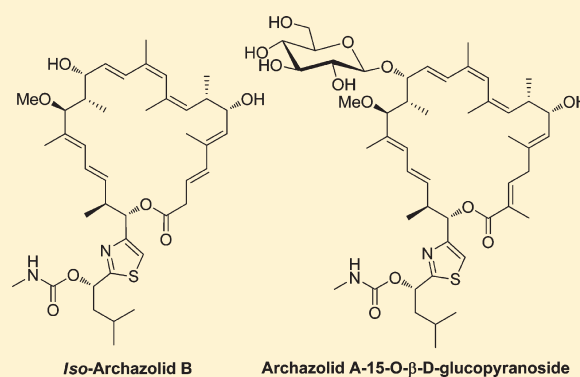
[†]Institut für Organische Chemie, Ruprecht-Karls-Universität Heidelberg, Im Neuenheimer Feld 270, D-69120 Heidelberg, Germany

[‡]Helmholtz-Zentrum für Infektionsforschung, Medizinische Chemie and ^{||}Chemische Biologie, Inhoffenstrasse 7, D-38124 Braunschweig, Germany

[§]Fachbereich Biologie/Chemie, Abteilung Tierphysiologie, Universität Osnabrück, D-49069 Osnabrück, Germany

S Supporting Information

ABSTRACT: Two structurally novel analogues of the macrolides archazolid A and B, archazolid A-15-O- β -D-glucopyranoside (archazolid E, **5**) and *iso*-archazolid B (archazolid F, **6**), were isolated from the myxobacterium *Cystobacter violaceus* and *Archangium gephyra*, respectively. Macrolactone **5** represents the first 15-O-glycoside of the archazolids. *iso*-Archazolid B (**6**) incorporates a C-3 alkene and presents the first constitutional isomer reported for this natural product class. The structures of these polyketides were determined by spectroscopic analysis, in particular by HMBC, HMQC, and ROESY NMR investigations and by chemical degradation. *iso*-Archazolid B (**6**) demonstrated extremely high antiproliferative and V-ATPase inhibitory effects, with IC₅₀ values in the picomolar range, while only moderate activity was observed for glycoside **5**. *iso*-Archazolid B presents the most potent archazolid known.



Vacuolar type ATPases (V-ATPases) are a family of hetero-multimeric ATP-dependent ion pumps that energize transport processes, in particular of protons across membranes by hydrolysis of ATP.^{1–3} Intracellular V-ATPases are involved in various cellular processes, including receptor-mediated endocytosis,⁴ intracellular membrane traffic, processing of pro-hormones, degradation of proteins, and release of neurotransmitters.⁵ Furthermore, plasma membrane V-ATPases have critical functions in different physiological processes such as urinary acidification,^{6,7} bone resorption,⁸ and sperm maturation.⁹ V-ATPases are associated with various human diseases, including osteoporosis, tubular acidosis, tumor metastasis, infection by influenza and other viruses, and bacterial infections by anthrax or diphtheria¹⁰ and have an increasingly emerging potential as drug targets.^{11–13} This renders the development and molecular understanding of potent V-ATPase inhibitors important research goals.

In the late 1990s, the polyketide macrolide archazolid A (**1**) and B (**2**) were reported from the myxobacterium *Archangium gephyra* by the groups of Höfle and Reichenbach.^{14,15} With activities in the low nanomolar region *in vitro* and *in vivo*, they are among the most potent V-ATPase inhibitors known.^{14,16,17} On a molecular level, they selectively target V-ATPases, which adds to their attractiveness for further development. Archazolid

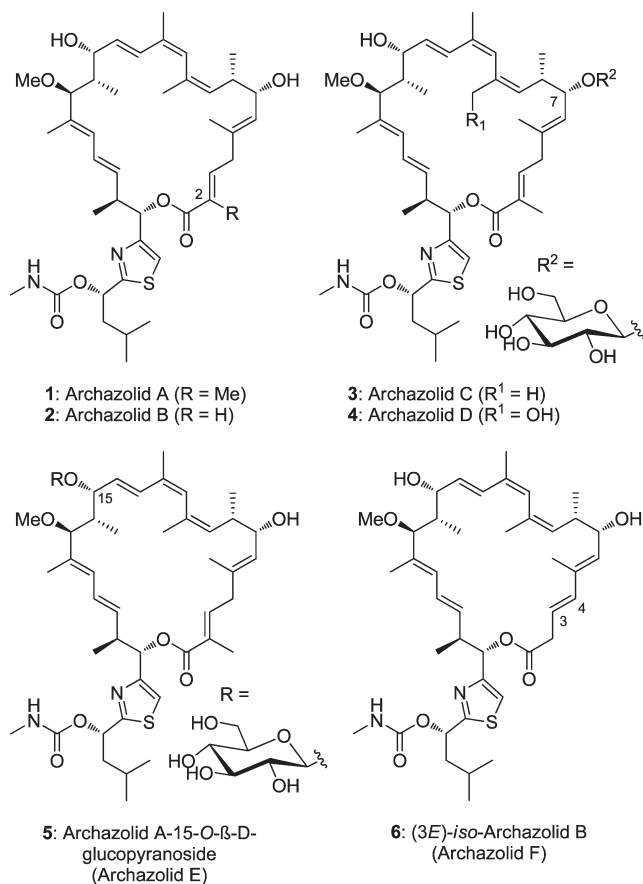
A (**1**) has been shown to bind to the V_O subunit c in a noncovalent manner.¹⁷ Multiple copies of subunit c form a ring, the structure of which was analyzed by X-ray crystallography at a resolution of 2.1 Å in a bacterial homologue,¹⁸ and subsequently the structure of the complete eukaryotic V-ATPase enzyme was determined by cryo-electron microscopy with a resolution of 16.5 Å.¹⁹ Very recently, the binding site in this subunit has been analyzed in more detail by cross-linking experiments of an archazolid A derivative in combination with site-directed mutagenesis studies of the protein, demonstrating that archazolid A (**1**) binds to the equatorial region of the c-ring.²⁰ While the archazolids were originally isolated from *Archangium gephyra*, more recent reports have indicated that the myxobacterium *Cystobacter violaceus* produces a greater diversity of archazolids, and two other derivatives, archazolid C (**3**)²¹ and archazolid D (**4**), with glucosides at C-7 (**3** and **4**) and an additional hydroxyl group (**4**),²² have been isolated from this myxobacterium.

While the archazolids were originally reported as planar structures, their absolute and relative stereochemistry was determined in 2006 by high-field NMR studies in combination with

Received: January 12, 2011

Published: April 22, 2011

molecular modeling and derivatization²³ and subsequently confirmed by total syntheses of archazolids A (1)^{24,25} and B (2).²⁶ So far only a limited number of SAR studies on synthetic²⁷ and natural analogues^{21,22} have been reported; this will be critical in advancing these macrolide antibiotics and may help in deriving a better molecular understanding of the function of the V-ATPase enzyme.²⁸ Herein, we describe the isolation, structure elucidation, and biological evaluation of two structurally novel archazolid derivatives, archazolid A-15-*O*- β -D-glucopyranoside (archazolid E, 5) and *iso*-archazolid B (archazolid F, 6), from the myxobacterium *Cystobacter violaceus* and *Archangium gephyra*, respectively.



RESULTS AND DISCUSSION

In the course of previous studies²⁷ the myxobacterium *Cystobacter violaceus* strain Cb vi105²² has been identified as an efficient source for structurally novel archazolid derivatives, while *Archangium gephyra* strain Ar 3548¹⁶ was a more productive source for archazolids A (1) and B (2). In order to study minor natural archazolid derivatives, each of these organisms was cultivated in 350 L bioreactors with 300 L of medium in the presence of Amberlite XAD-16 (1%) for adsorption. In a similar fashion, the adsorber resin and cell mass were harvested after 10 days by centrifugation and extracted with acetone to give a crude extract. A detailed HPLC-MS analysis of these crude mixtures in combination with the characteristic UV-vis spectra of the archazolids (maximum 238/239 nm) suggested the presence of at least one novel derivative in both fermentation broths. Consecutive purification by gel chromatography (Sephadex LH-20), MPLC, and finally reversed-phase HPLC gave the novel metabolites archazolid A-15-*O*- β -D-glucopyranoside (archazolid F, 5,

1.0 mg yield; apparent yield <0.0035 mg/L) from *Cystobacter violaceus* strain Cb vi105 and *iso*-archazolid B (archazolid E, 6, 1.5 mg yield; apparent yield <0.005 mg/L) from *Archangium gephyra* strain Ar 3548.

The close similarity of the ¹H NMR, ¹³C NMR, and two-dimensional NMR spectra of these two novel metabolites suggested core structures closely related to those of the parent natural products archazolids A (1) (Table 1) and B (2). Together with the ¹³C NMR spectra and HRMS analysis of the novel metabolite 5, indicating the molecular formula to be C₄₈H₇₂N₂O₁₂S, corresponding to 162 mass units (i.e., C₆H₁₀O₅) higher than archazolid A (1), the data suggest this macrolide to be a hexose of archazolid A (1). The *O*-glycosidic nature of this compound also became evident from a doublet at δ 4.22 (7.7 Hz), attributed to an anomeric proton (1'''-H). The signals for 2'''-H to 5'''-H were resolved in CD₃OD and assigned to glucose. The ¹³C NMR data also displayed the expected number of carbons and chemical shifts for glucose. The position of the glucose unit was further confirmed by ROESY experiments, which showed interactions of H-1''' with H-14, and by long-range C-H correlation from 1'''-H to C-15 and from H-15 to C-1'''. Therefore, the sugar unit is situated at position C-15, and the new glycoside has the constitution shown in Figure 1. Its structure was further confirmed by TOCSY experiments and HMBC and HMQC interactions. Further proof of its constitution was obtained by hydrolysis and GC-/HPLC comparison with an authentic sample of glucose. For the new glycoside, we suggest the name archazolid E (5).

The ¹H NMR spectrum of the novel metabolite 6 from *Archangium gephyra* likewise showed characteristic ¹H NMR patterns of the archazolid core (Table 1). However, in contrast to archazolid A (1), a methyl group at C-2 was missing, which together with HRMS data (molecular formula C₄₁H₆₀N₂O₇S) suggested 6 to be an isomer of archazolid B (2). Crucial in deducing the structure of the novel metabolite was a doublet for H-4 in the olefinic region [δ 6.21 ppm (*J* = 15.4 Hz)], one doublet of a triplet for H-3 [δ 5.81 ppm (*J* = 15.4, 7.3 Hz)], and the appearance of the H-2 protons in the aliphatic region [δ 3.17, d (*J* = 15.4, 7.3 Hz)]. Consequently, this novel derivative bears a double bond between C-3 and C-4 as shown, instead of an alkene between C-2 and C-3. The *E*-configuration of the double bond was assigned on the basis of the size of the coupling constant (15.4 Hz) and NOE data, as shown in Figure 2. The structure of this novel macrolide was confirmed by HMBC correlation as well as HSQC data.²⁹

Previous feeding studies with ¹³C-enriched acetate and methionine to *Archangium gephyra* have shown that the macrocyclic core of archazolid A, with the exception of C-23, is derived from these building blocks.^{23,30} As shown in Figure 3 for archazolid B, the 5*E*,9*Z*,11*Z*,13*E* olefinic double bonds are within these acetate or propionate fragments and not between these building blocks, as commonly observed in polyketide biosynthesis (viz., 18*E* and 20*E* alkenes). This may suggest a flexible dehydratase domain or more likely an isomerization process. The occurrence of the double-bond isomers archazolid B (2) and *iso*-archazolid B (6) may also originate from a migration of the 2,3-double bond (archazolid B) to the unusual 3,4-position in *iso*-archazolid B (6) during the biosynthesis of these macrolides.

For biological evaluation of the analogues, their inhibitory effect on the growth of the mammalian murine tissue cell line L-929 was evaluated, in direct comparison with archazolids A, B, C, and D (Table 2). Archazolid A-15-*O*- β -D-glucopyranoside

Table 1. NMR Data for Archazolid A (1), Archazolid A-15-O- β -D-glucopyranoside (archazolid E, 5) and iso-Archazolid B (archazolid F, 6) in CD₃OD^a

position	archazolid A (1)		archazolid A-15-O- β -D-glucopyranoside (archazolid E, 5)		iso-archazolid B (archazolid F, 6)	
	δ_C	δ_H mult. (J in Hz)	δ_C	δ_H mult. (J in Hz)	δ_C	δ_H mult. (J in Hz)
1	168.3		168.5		172.5	
2	129.7		123.0		39.6	3.17d (7.3)
3	142.1	6.82 ddd (7.9, 7.5, 1.3)	142.3	6.81 t (7.5)	121.7	5.81 dt (15.4, 7.3)
4	40.6	2.91 dd (15.0, 7.5) 3.03 dd (15.0, 7.5)	40.9	2.93 dd (14.3, 7.0)/ 3.04 dd (14.7, 8.1)	139.7	6.21 d (15.4)
5	136.9		137.5		134.8	
6	130.4	5.21 dd (9.5, 1.2)	130.8	5.21 d (9.2)	134.8	5.33 d (8.8)
7	73.6	4.03 dd (9.4, 9.3)	73.9	4.04 t (9.5)	73.3	4.13 t (9.2)
8	41.6	2.30 ddq (9.5, 9.8, 7.0)	41.7	2.32 m	41.5	2.36 ddq (9.5, 9.5, 6.6)
9	132.7	5.27 d (9.6)	132.6	5.29 d (9.5)	132.3	5.26 d (9.9)
10	134.8		135.0		134.6	
11	130.8	5.81 d (1.0)	131.2	5.80 s	130.6	5.77 s
12	133.6		133.5		133.1	
13	129.3	6.56 dd (15.5, 0.9)	131.3	6.73 d (14.3)	129.2	6.56 d (15.8)
14	133.6	5.79 dd (15.5, 6.0)	130.9	5.73 dd (16.1, 6.2)	133.4	5.83 m ^b
15	75.5	4.31 dd (6.4, 3.2)	80.6	4.60 m	75.8	4.28 brs
16	44.5	1.80 ddq (9.0, 7.0, 3.2)	44.0	1.75 m	43.8	1.76 m
17	89.8	3.40 d (9.0)	89.0	3.47 d (6.6)	89.9	3.34 d (9.3)
18	135.7		136.2		135.8	
19	129.9	5.87 dd (10.9, 1.2)	130.1	5.87 d (10.6)	130.0	5.81 d (11.1)
20	127.6	6.17 dd (15.5, 10.9)	127.8	6.16 dd (13.0, 12.3)	127.3	6.22 dd (15.0, 10.9)
21	135.1	5.63 dd (15.2, 7.0)	134.8	5.59 dd (15.2, 6.8)	135.2	5.59 dd (15.4, 7.3)
22	42.0	3.10 ddq (7.5, 7.0, 4.0)	42.0	3.12 dd (10.1, 6.1)	41.5	3.06 qdd (7.2, 6.6, 5.8)
23	77.6	5.97 d (4.1)	77.8	6.02 d (3.3)	72.3	5.85 dd (6.6, 1.8)
Me-2	12.6	1.91 d (1.2)	12.8	1.93 s		
Me-5	16.8	1.73 d (1.2)	16.8	1.75 d (1.1)	13.3	1.87 d (0.7)
Me-8	17.7	0.84 d (7.0)	17.9	0.85 d (6.6)	17.8	0.87 d (6.6)
Me-10	24.7	1.80 brs	24.9	1.80 s	24.8	1.82 s
Me-12	19.9	1.93 d (1.2)	20.0	1.95 d (1.1)	20.1	1.95 d (1.1)
Me-16	12.6	0.74 d (7.0)	12.9	0.78 d (7.0)	12.8	0.73 d (7.3)
OMe-17	56.2	3.16 s	56.2	3.18 s	56.0	3.16 s
Me-18	13.0	1.64 d (1.2)	12.9	1.64 s	12.2	1.64 s
Me-22	17.6	1.15 d (7.0)	17.5	1.22 d (7.0)	17.2	1.07 d (7.0)
1'	73.3	6.04 dd (9.1, 4.5)	73.5	6.05 dd (9.2, 4.8)	73.2	6.03 dd (9.2, 4.4)
2'	173.9		174.1		174.2	
3'	156.1		156.3		155.4	
4'	116.7	7.21 s	116.6	7.18 s	117.5	7.29 s
5'	46.0	1.92 m	46.1	1.86 m/1.93 m	45.9	1.91 m/1.82 m
6'	25.8	1.77 m	26.0	1.81 m	24.8	1.78 m
7'	23.4	1.01 d (6.0)	23.5	1.04 d (6.6)	23.2	1.02 d (7.0)
8'	22.4	1.02 d (6.0)	22.5	1.05 d (6.6)	23.2	1.03 d (6.6)
1''	158.2		158.4		158.3	
2''	27.5	2.75 s	27.7	2.76 s	27.4	2.75 s
1'''			102.0	4.27 d (7.7)		
2'''			75.3	3.28 ddd (12.1, 8.8, 5.5)		
3'''			78.1	3.39 m		
4'''			77.9	3.22 ddt (7.2, 5.0, 2.3)		
5'''			71.9	3.39 m		
6'''			62.9	3.75 dd (11.7, 5.5)/3.89 dd (11.7, 2.6)		

^a Recorded at 600 MHz (¹H) and 150 MHz (¹³C). ^b The coupling constants for H-14 could be deduced in *d*₆-acetone: δ 5.79 ppm, dd, (*J* = 16.1, 4.1 Hz).

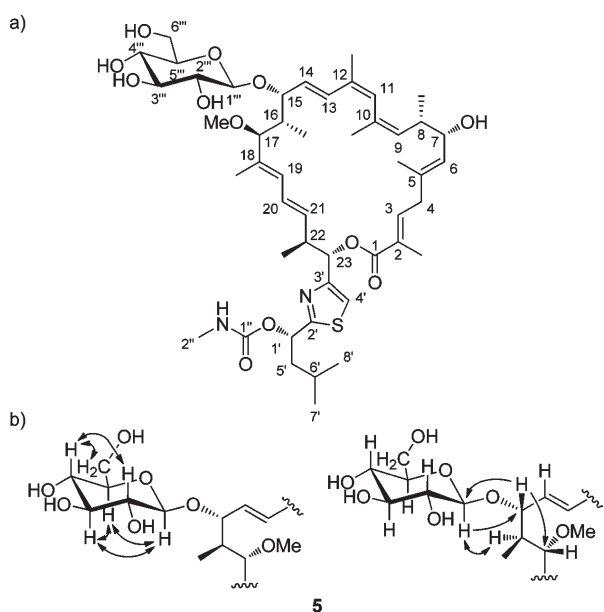


Figure 1. Archazolid A-15-*O*-β-D-glucopyranoside (archazolid E, 5): numbering of atoms (a) as well as HMBC (single arrows) and ROESY interactions (double arrows) (b).

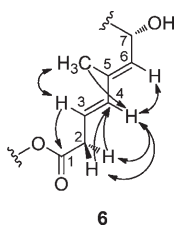


Figure 2. HMBC (single arrows) and ROESY interactions (double arrows) for the C-1 to C-7 subunit of 6.

demonstrated antiproliferative activities with submicromolar concentrations ($IC_{50} = 0.51 \mu M$). It was less potent than the parent natural product archazolid A (1), but three times more active than the corresponding 7-*O*-β-glucosylated archazolid (3) ($IC_{50} = 1.6 \mu M$).²⁷ This may suggest that the 15-OH might not be as important for binding compared with the hydroxyl at C-7; this is in agreement with previous data obtained for a 15-oxo derivative.²⁷ Together with previous data these results suggest the fragment between C-7 and C-15 to be part of the pharmacophore region of these macrolide antibiotics. *iso*-Archazolid B (6), in contrast, demonstrated extremely potent antiproliferative activity, with an IC_{50} value in the subnanomolar range, which is around 10 times more active than archazolids A (1) and B (2). Notably, it is the most potent archazolid known. *iso*-Archazolid B (6) was also evaluated for inhibition of purified V-ATPase holoenzyme from the midgut of the tobacco hornworm *Manduca sexta*. Likewise, it demonstrated extremely high potency in this *in vitro* test, comparable to that of archazolids A (1) and B (2). These data indicate that a certain degree of structural flexibility in the C-1 to C-4 region is possible while retaining the biological potency. The observation that archazolid F is equipotent to archazolids A and B in the enzyme assay but has a much more pronounced antiproliferative activity is noteworthy and may suggest a different biological availability and/or possibly also another

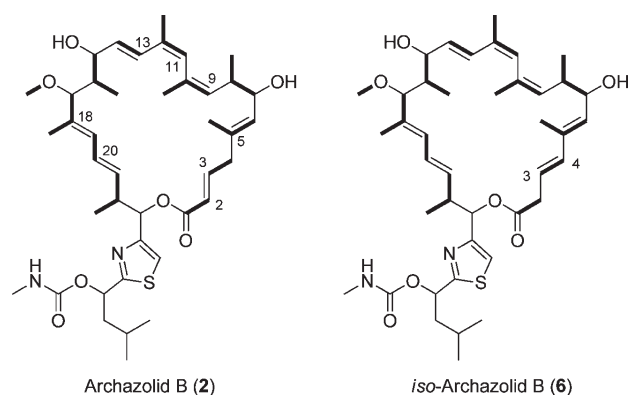


Figure 3. Biosynthetic origin of archazolid B (2) and *iso*-archazolid B (6), in analogy with the biosynthesis of archazolid A (C-methyl groups may originate from methionine or methyl-malonyl-CoA).²³

Table 2. Inhibition of the V_1/V_0 Holoenzyme Activity and Cytotoxicity of the Archazolids

	enzyme inhibition	
	V_1/V_0 holoenzyme: IC_{50} [nmol/mg enzyme] ^d	growth inhibition L-929: IC_{50} [nM] ^g
archazolid A (1)	0.6 ^b	0.81
archazolid B (2)	0.6 ^c	1.1
archazolid C (3)	210 ^d	1600 ^d
archazolid D (4)	1200 ^e	330 ^e
archazolid E (5)	n.d. ^f	510
archazolid F (6)	0.7	0.11

^aThe specific enzyme activity of the controls without inhibitors was approximately $1.5 \mu mol mg^{-1} min^{-1}$. ^b0.8 nmol/mg enzyme accords to 10 nM. ^cValue taken from ref 17. ^dValue taken from ref 22. ^eValue taken from ref 21. ^fn.d.: not determined. ^gOrigin of the mammalian cell line: Murine connective tissue DSM ACC 2.

biological target. Notably, the solution conformation of archazolid A (1)^{23,31} in this region closely resembles that of an *E*-configured C-3 alkene, as present in *iso*-archazolid B (6), which may indicate that the solution conformation of this structural domain also correlates to the bioactive conformation.

Because of the extremely potent cytotoxic activity of archazolid F against cell line L-929, it was further evaluated against a range of other cancer cell lines. As shown in Table 3, archazolid F showed extreme potency in all cases, with IC_{50} values in the picomolar range. Furthermore, a certain degree of selectivity was observed for specific cell lines, which might be important for the future development of archazolids as chemotherapeutic agents.

EXPERIMENTAL SECTION

General Experimental Procedures. Optical rotations were determined on a Perkin-Elmer 241 instrument. UV spectra were recorded on a Shimadzu UV-2102 PC scanning spectrometer. IR spectra were measured with a Nicolet 20DXB FT-IR spectrometer. NMR spectra were recorded in CD_3OD and $CO(CD_3)_2$ on a Bruker DMX-600 and a Bruker WM-400 spectrometer. ESI+ and DCI mass spectra (reactant gas ammonia) were obtained on a Bruker ICR APEX-QE spectrometer; high-resolution data were acquired using peak matching ($M/DM = 10000$). Pure compounds were characterized by analytical HPLC on a Nucleosil C_{18} (column: $125 \times 2 mm$, $5 \mu m$, flow rate: $0.3 mL/min$), with diode array detection. Preparative HPLC was carried

Table 3. Antiproliferative Activity of Archazolid F against Various Cell Lines

cell line	type of cell line	growth inhibition: IC ₅₀ [nM] of archazolid F
L-929	mouse fibroblasts	0.107
KB-3-1	human cervix carcinoma	0.042
U-937	human histiocytic lymphoma	0.038
A-431	human epidermoid carcinoma	0.043
SK-OV-3	human ovary adenocarcinoma	0.111
PC-3	prostate adenocarcinoma	0.053
MCF7	breast adenocarcinoma	0.131

out on an Agilent Technologies 1200 Series from Agilent with a Nucleosil column (250 × 21 mm, 5 μm, flow rate: 18 mL/min, detection: UV absorption at 254 nm) from Machery, Nagel & Co. Analytical TLC was performed with TLC aluminum sheets, silica gel Si 60 F₂₅₄ (Merck), solvent: mixtures of ethylacetate/petroleum ether, detection: UV absorption at 254 nm, dark blue spots on staining with cerium-(IV)sulfate-phosphomolybdic acid in sulfuric acid followed by charring.

Culture Conditions, Production, and Isolation of Archazolid A-15-O-β-D-glucopyranoside (archazolid E, 5). For isolation of archazolid E (5) from *Cystobacter violaceus*, a 300 L fermentation batch of strain Cb vi105, isolated at the HZI, was grown in M7 medium in the presence of 3 L of Amberlite XAD-16 adsorber resin at 30 °C.¹⁷ After harvesting by centrifugation, the mixture of wet cell mass and adsorber resin was extracted with acetone (4 × 4 L) by stirring, sedimentation, and decanting. Evaporation gave the crude extract (13.7 g), which was dissolved in methanol for further purification by gel chromatography on Sephadex LH 20 (Fluka Steinheim, solvent: methanol, flow rate: 7 mL/min). Further purification by medium-pressure RP chromatography (solvent: methanol/water, 85:15, detection 230 nm, flow rate: 55 mL/min) and HPLC (solvent: acetonitrile/water, 63:37, detection 254 nm diode array, flow rate: 15 mL/min) gave archazolid E (5) (1.5 mg) together with other archazolids as previously reported.²²

Culture Conditions, Production, and Isolation of iso-Archazolid B (archazolid F, 6). *Archangium gephyra*, strain Ar 3548, isolated at the HZI, was cultured for 10 days at 30 °C in a 350 L bioreactor with 300 L of medium in the presence of 3 L of Amberlite XAD-16 adsorber resin, according to the previously reported procedure.¹⁶ XAD-16 adsorber resin was thoroughly eluted with acetone (4 × 4 L). The acetone was evaporated *in vacuo* followed by distribution of the residue between water and ethyl acetate. The organic layer was separated and concentrated *in vacuo*. The residue was dissolved in methanol, washed three times with heptane, and filtered through a silica plug. Evaporation gave the crude extract (26.1 g), which was dissolved in methanol for further purification by gel chromatography on Sephadex LH 20 (Fluka Steinheim, solvent: methanol, flow rate: 7 mL/min). Further purification by medium-pressure RP chromatography (solvent: methanol/water, 8:2, detection 230 nm, flow rate: 65 mL/min) and high-pressure RP chromatography (solvent: acetonitrile/water, 65:35, detection 230 nm diode array, flow rate: 15 mL/min) gave archazolid F (6) (1.0 mg) together with other archazolids as previously reported.¹⁶

Physicochemical Properties of Archazolid E (5): colorless oil. [α]_D²⁵ −37.89 (c 0.57, MeOH); λ_{max} (log ε) 239 nm (4.9); NMR data, see Table 1; HRMS (ESI) for C₄₈H₇₂N₂O₁₂NaS [M + Na]⁺ calcd m/z 923.4704, found m/z 923.4711.

Hydrolysis of Archazolid E. Glucose was detected as the per-TMS-silylated methyl-glycoside according to the method of Chaplin.³²

Physicochemical properties of archazolid F (6): colorless oil; [α]_D²⁵ −25.0 (c 0.11, MeOH); λ_{max} (log ε) 238 nm (4.9); IR (film) ν_{max} 2931, 2889, 2361, 1602, 1019 cm^{−1}; NMR data, see Table 1;

HRMS (ESI) for C₄₁H₆₀N₂O₇NaS [M + Na]⁺ calcd 747.4018, found 747.4012; HRMS for C₄₁H₆₀N₂O₇KS [M + K]⁺ calcd m/z 763.3758, found m/z 763.3752.

Cell Culture and Growth Inhibition Assay. The L-929 mouse cell line was from the German Collection of Microorganisms and Cell Cultures (DSMZ) and cultivated in DME medium (Gibco BRL) plus 10% newborn calf serum at 37 °C and 10% CO₂ in a moist atmosphere. Growth inhibition was measured on microtiterplates. Aliquots of 120 μL of the suspended cells (50 000 mL^{−1}) were added to 60 μL of a serial dilution of the inhibitor. After 5 days, metabolic activity per well was determined using the MTT assay.³³ The results were related to control wells, which were incubated with only the vehicle methanol. These were set to 100%.

V-ATPase Assays. V-ATPase was purified according to published procedures.³⁴ Standard V-ATPase assays with a final volume of 160 μL and a pH of 8.1 consisted of 3 μg of protein, 50 mM Tris-MOPS, 3 mM 2-mercaptoethanol, 1 mM MgCl₂, 20 mM KCl, 0.003% C₁₂E₁₀, 20 mM NaCl, and 3 mM Tris-HCl. After 5 min of preincubation at 30 °C with or without inhibitors, 1 mM Tris-ATP was added, and after incubation for 2 min, the reaction was stopped by placing the tube in liquid nitrogen. As a control, the inhibition of the V-ATPase activity by the established inhibitor archazolid A was tested in parallel assays.¹⁷ Inorganic phosphate produced in the assays of V-ATPase was measured according to the protocol of Wiczorek et al.³⁵ (Table 2).

■ ASSOCIATED CONTENT

Supporting Information. Copies of NMR spectra for archazolid E (5) and archazolid F (6). This material is available free of charge via the Internet at <http://pubs.acs.org>.

■ AUTHOR INFORMATION

Corresponding Author

*Phone: +49 6221 546207. Fax: + +49 6221 544205. E-mail: dirk.menche@oci.uni-heidelberg.de.

■ ACKNOWLEDGMENT

This work was generously supported by the Volkswagenstiftung (Funding Initiative: “Interplay between Molecular Conformations and Biological Function”), the Fonds der Chemischen Industrie (Stipendium to S.E.), and the “Wild-Stiftung”. We thank T. Arnold, W. Collisi, and E. Persch for technical support and the Fermentation Service of the HZI for help with large-scale fermentation. Particular thanks are also due to Dr. M. Nimtz (HZI, Braunschweig) for GC-MS analysis of glucose.

■ REFERENCES

- (1) Beyenbach, K. W.; Wiczorek, H. *J. Exp. Biol.* **2006**, *209*, 577–589.
- (2) Nishi, T.; Forgac, M. *Nat. Rev. Mol. Cell Biol.* **2002**, *3*, 94–103.
- (3) Jefferies, K. C.; Cipriano, D. J.; Forgac, M. *Arch. Biochem. Biophys.* **2008**, *476*, 33–42.
- (4) Maxfield, F. R.; McGraw, T. E. *Nat. Rev. Mol. Cell Biol.* **2004**, *5*, 121–132.
- (5) Hiesinger, P. R.; Fayyazuddin, A.; Mehta, S. Q.; Rosenmund, T.; Schulze, K. L.; Zhai, R. G.; Verstreken, P.; Cao, Y.; Zhou, Y.; Kunz, J.; Bellen, H. J. *Cell* **2005**, *121*, 607–620.
- (6) Wagner, C. A.; Finberg, K. E.; Breton, S.; Marshansky, V.; Brown, D.; Geibel, J. P. *Physiol. Rev.* **2004**, *84*, 1263–1314.
- (7) Brown, D.; Paunescu, T. G.; Breton, S.; Marshansky, V. *J. Exp. Biol.* **2009**, *212*, 1762–1772.
- (8) Toyomura, T.; Murata, Y.; Yamamoto, A.; Oka, T.; Sun-Wada, G. H.; Wada, Y.; Futai, M. *J. Biol. Chem.* **2003**, *278*, 22023–22030.

- (9) Pietrement, C.; Sun-Wada, G. H.; Silva, N. D.; McKee, M.; Marshansky, V.; Brown, D.; Futai, M.; Breton, S. *Biol. Reprod.* **2006**, *74*, 185–194.
- (10) Forgac, M. *Nat. Rev. Mol. Cell Biol.* **2007**, *8*, 917–929.
- (11) Niikura, K. *Drug News Perspect.* **2006**, *19*, 139–144.
- (12) Perez-Sayans, M.; Somoza-Martin, J. M.; Barros-Angueira, F.; Rey, J. M.; Garcia-Garcia, A. *Cancer Treat. Rev.* **2009**, *35*, 707–713.
- (13) Huss, M.; Wieczorek, H. *J. Exp. Biol.* **2009**, *212*, 341–346.
- (14) Höfle, G. R., H.; Sasse, F.; Steinmetz, H. German Patent DE 41 42 951 C1, 1993.
- (15) For general reviews on polyketides from myxobacteria, see: (a) Menche, D. *Nat. Prod. Rep.* **2008**, *25*, 905–918. (b) Weissman, K. J.; Müller, R. *Nat. Prod. Rep.* **2010**, *27*, 1276–1295.
- (16) Sasse, F.; Steinmetz, H.; Hofle, G.; Reichenbach, H. *J. Antibiot.* **2003**, *56*, 520–525.
- (17) Huss, M.; Sasse, F.; Kunze, B.; Jansen, R.; Steinmetz, H.; Ingenhorst, G.; Zeeck, A.; Wieczorek, H. *BMC Biochem.* **2005**, *6*, 13.
- (18) Murata, T.; Yamato, I.; Kakinuma, Y.; Leslie, A. G.; Walker, J. E. *Science* **2005**, *308*, 654–659.
- (19) Muench, S. P.; Huss, M.; Song, C. F.; Phillips, C.; Wieczorek, H.; Trinick, J.; Harrison, M. A. *J. Mol. Biol.* **2009**, *386*, 989–999.
- (20) Bockelmann, S.; Menche, D.; Rudolph, S.; Bender, T.; Grond, S.; von Zezschwitz, P.; Muench, S. P.; Wieczorek, H.; Huss, M. *J. Biol. Chem.* **2010**, *285*, 38304–38314.
- (21) Menche, D.; Hassfeld, J.; Steinmetz, H.; Huss, M.; Wieczorek, H.; Sasse, F. *J. Antibiot.* **2007**, *60*, 328–331.
- (22) Menche, D.; Hassfeld, J.; Steinmetz, H.; Huss, M.; Wieczorek, H.; Sasse, F. *Eur. J. Org. Chem.* **2007**, 1196–1202.
- (23) Hassfeld, J.; Farès, C.; Steinmetz, H.; Carlomagno, T.; Menche, D. *Org. Lett.* **2006**, *8*, 4751–4754.
- (24) Menche, D.; Hassfeld, J.; Li, J.; Rudolph, S. *J. Am. Chem. Soc.* **2007**, *129*, 6100–6101.
- (25) Menche, D.; Hassfeld, J.; Li, J.; Mayer, K.; Rudolph, S. *J. Org. Chem.* **2009**, *74*, 7220–7229.
- (26) Roethle, P. A.; Chen, I. T.; Trauner, D. *J. Am. Chem. Soc.* **2007**, *129*, 8960–8961.
- (27) Menche, D.; Hassfeld, J.; Sasse, F.; Huss, M.; Wieczorek, H. *Bioorg. Med. Chem. Lett.* **2007**, *17*, 1732–1735.
- (28) Saroussi, S.; Nelson, N. *J. Exp. Biol.* **2009**, *212*, 1604–1610.
- (29) *iso*-Archazolid B (**6**) can be detected directly in the fermentation broth before isolation, which suggests that it presents an authentic natural product and not an isolation artifact derived from archazolid B. Isomerization during extraction or detection likewise seems highly unlikely, as this has never been detected for the archazolid family under such conditions (see refs 16, 21–27). A related double-bond migration has been observed only for a ring-opened derivative but not for the macrocyclic metabolites. Also, this isomerization has occurred only under basic conditions but not under the neutral pH values present during fermentation (see ref 23). Therefore an isomerization is much more likely before ring-closure, i.e., during the biosynthesis of *iso*-archazolid B.
- (30) For leading references on the biosynthesis of myxobacterial polyketides and polyketides in general, see: (a) Staunton, J.; Weissman, K. J. *Nat. Prod. Rep.* **2001**, *18*, 380–416. (b) Wenzel, S. C.; Muller, R. *Nat. Prod. Rep.* **2009**, *26*, 1385–1407. (c) Hertweck, C. *Angew. Chem., Int. Ed.* **2009**, *48*, 4688–4716.
- (31) Fares, C.; Hassfeld, J.; Menche, D.; Carlomagno, T. *Angew. Chem., Int. Ed.* **2008**, *47*, 3722–3726.
- (32) Chaplin, M. F. *Anal. Biochem.* **1982**, *123*, 336–341.
- (33) Mosmann, T. *J. Immunol. Methods* **1983**, *65*, 55–63.
- (34) Huss, M.; Ingenhorst, G.; König, S.; Gassel, M.; Drose, S.; Zeeck, A.; Altendorf, K.; Wieczorek, H. *J. Biol. Chem.* **2002**, *277*, 40544–40548.
- (35) Wieczorek, H.; Cioffi, M.; Klein, U.; Harvey, W. R.; Schweikl, H.; Wolfersberger, M. G. *Methods Enzymol.* **1990**, *192*, 608–616.